

Preparation of Fe-N-Carbon Nanocoils as Catalyst for Oxygen Reduction Reaction

Shuihua Tang^{1,2,*}, Haixin Huangfu^{1,2}, Zhen Dai^{1,2}, Leping Sui^{1,2}, Zhentao Zhu^{1,2}

¹ State Key Laboratory of Oil and Gas Reservoir Geology & Exploitation, Southwest Petroleum University, Chengdu 610500, China

² School of Materials and Engineering, Southwest Petroleum University, Chengdu 610500, China

*E-mail: shuihuatang@swpu.edu.cn

Received: 27 May 2015 / Accepted: 4 July 2015 / Published: 28 July 2015

Carbon nanocoil (CNC) with large specific surface area of $398 \text{ m}^2\text{g}^{-1}$ was synthesized by heat-treatment of resorcinol and formaldehyde resin, and Fe-N-CNC and Fe-N-XC72 catalysts with variously nominal Fe contents were prepared by carbonization of in-situ polymerized polyaniline in the presence of CNC or XC72 and Fe species. The Fe-N-C catalysts were characterized by Fourier Transformation Infrared Spectroscopy, X-ray Photoelectron Spectroscopy, Transmission Electron Microscopy, and then oxygen reduction reaction (ORR) activity and stability were determined by cyclic voltammetry (CV) and linear sweep voltammetry. Fe-N-CNC catalyst with Fe nominal content of 5 wt% indicates more pyridinic and graphitic nitrogen, less pyrrolic nitrogen and total N/C ratio, it also demonstrates 30 mV more positive of half-wave potential compared to Fe-N-XC72 catalyst, and after 1000 CV cycles at scan rate of 50 mVs^{-1} , the half-wave potential of Fe-N-CNC cathodically shifts 20 mV respect to 40 mV of Fe-N-XC72. This is mainly due to CNC with unique morphology and higher electron conductivity, which facilitate oxygen transportation and further reduction reaction. The ORR activities indicate that the type of nitrogen incorporating in carbon is far more important than the total content of nitrogen.

Keywords: Carbon nanocoil, polyaniline, non-precious metal catalyst, oxygen reduction reaction

1. INTRODUCTION

Thanks to high efficiency, low operation temperature, and low environmental impact, proton exchange membrane fuel cell (PEMFC) has been regarded as one of the most promising energy conversion technologies today. However, commercialization of PEMFC confronts a big challenge—high cost originated from expensive catalysts, because platinum or platinum alloy based catalyst is mostly used as anode or cathode catalyst. Therefore, non-precious metal catalysts (NPMCs) have been

extensively studied, especially cathode catalyst for oxygen reduction reaction (ORR), such as transition metal carbides, transition metal oxides, macrocycle-based catalysts, and M-N-C (M=Fe and/or Co) catalysts [1-3]. Among them, M-N-C catalyst is considered as one of the most promising candidate due to its high activity, remarkable performance stability, and low cost [4-10]. Jasinski found that cobalt phthalocyanine could catalyze oxygen reduction reaction in 1964 [4], after that numerous efforts to synthesize high active non-precious metal catalysts for ORR have been made. Dodelet et al prepared highly active NPMCs via ball milling a mixture containing carbon support, phenanthroline, and iron acetate, and then heat treated under an inert atmosphere [6]. Although this kind of catalyst offered good ORR activity, it suffered from poor stability in an acidic environment. Later in 2011, Wu et al also synthesized M-N-C catalysts using polyaniline (PANI) as nitrogen source, Ketjen Black as carbon support, and FeCl_3 as transition metal precursor, the catalysts demonstrated high activity, remarkable performance stability, as well as excellent four-electron selectivity [7].

For a certain M-N-C electrocatalyst, its ORR activity is determined by metal precursor, nitrogen source, carbon support, and synthesis conditions [11]. Carbon support affects not only active site distribution, but also mass transportation and electron conductivity, therefore its physicochemical properties and morphology play important roles in ORR activity of a catalyst. Carbon material with large specific surface area, high degree of graphitization, and proper pore size are favorable to establish a well-maintained three-phase interface. Wu et al studied the ORR activities of catalysts prepared by different carbon materials such as Ketjen Black, Black Pearls, and multi-walled carbon nanotubes (MWNTs) as support, the results indicated that the MWNT supported non-precious metal catalyst showed an excellent stability [12]. Carbon nanocoil (CNC) with large specific area of $451 \text{ m}^2\text{g}^{-1}$, highly graphitic characteristic, and unique structure was first synthesized and successfully applied as electrode materials for the anode in direct methanol fuel cells (DMFCs) by Hyeon et al [13]. Recently Zhang et al also indicated that mixture of XC72, MWNTs, and CNC supported Pt catalyst can improve ORR activity significantly, mainly due to CNC with unique morphology, which can facilitate mass transportation and electron/proton transfer [14]. However, CNC supported non-precious metal catalyst for ORR has not been reported.

In this paper, carbon nanocoil as carbon support, polyaniline as both nitrogen and carbon source, FeCl_3 as carbonization catalyst, Fe-N-C catalyst with different nominal Fe contents will be prepared, and their ORR activity and stability will be investigated.

2. EXPERIMENTAL

2.1. Preparation of carbon nanocoil (CNC)

CNC was prepared using formaldehyde and resorcinol as carbon precursors, iron nitrate and trisodium citrate composite as catalyst for graphitization, and silica sol (Akzo Nobel chemicals Corp., particle size of $\text{SiO}_2 = 4 \text{ nm}$, density = 1.1 gcm^{-3}) as a template. In a typical approach, a certain amount of trisodium citrate and iron nitrate were dissolved in de-ionized water, silica sol was added under ultrasonic stirring, and then a required amount of resorcinol and formaldehyde were added in

sequence. The resultant mixture of de-ionized water/ iron nitrate/ trisodium citrate/ resorcinol/ formaldehyde/ silica with a molar ratio of 100:0.8:1:2:4:0.8, was cured at 85 °C for 3 h, then heated to 850 °C and maintained for 3 h in an argon flow. After that, the carbonized material was refluxed in 3 M NaOH aqueous solution to get rid of silica and in 5 M HNO₃ solution to get rid of other residuals such as iron nanoparticles and carbonaceous species. Finally, CNC was obtained after being filtered, washed, and dried up at 80 °C in a vacuum oven.

2.2. Synthesis of Fe-N-C electrocatalysts

Fe-N-C electrocatalyst was synthesized using polyaniline as both nitrogen and carbon source, CNC or Vulcan XC72 were used as carbon support with mass ratio 5:1 of aniline to CNC or XC72. In a typical approach, 0.5 mL aniline was added into 50 mL 0.5 M HCl, sequentially CNC or XC72 was added to form a suspension, then the suspension was put into an ice bath and kept below 5 °C, while an oxidant (ammonium peroxydisulfate, APS) and transition metal precursor (iron chloride, FeCl₃) were added, and the process of further continuously stir for 8 h to ensure completely polymerization of aniline. Then the obtained mixture was dried at 100 °C, heat treated at 900 °C in flowing argon gas for 1 h, followed by acid-leaching in 0.5 M H₂SO₄ solution to get rid of unstable and inactive species. Eventually, Fe-N-CNC or Fe-N-XC72 was obtained after being filtered, washed with de-ionized water, and dried up at 80 °C in a vacuum oven overnight.

2.3. Physical characterization

Nitrogen adsorption-desorption isotherms were recorded with Quantachrome Nova Automated Gas Sorption System to calculate Brunauer-Emmett-Teller (BET) specific surface areas. Various functional groups presented in the polymer PANI as well as the catalysts were identified by FTIR spectra obtained by a Nicolet 6700 FTIR spectrometer. TEM images were achieved using a JEOL JEM-2010F microscope operated at 200 kV. XPS of the catalysts were acquired with a Thermo Scientific ESCALAB 250Xi X-ray photoelectron spectrometer by using Al-K α source.

2.4. Electrochemical tests

ORR activity of catalyst was evaluated by cyclic voltammetry (CV) and linear sweep voltammetry (LSV) on a rotating disk electrode (RDE, Pine AFMSRCE 2762). The AutoLab Potentiostat 302N (Metrohm, Holland) with a three-electrode system was used to recorded electrochemical results. The catalyst loading was controlled at 0.6 mgcm⁻². A glassy carbon (GC) disk with an area of 0.196 cm² was used as working electrode. Pt wire and Ag/AgCl electrode were used as counter and reference electrodes, respectively. The catalyst ink was prepared in a brief way as follows, 25 μ L of Nafion[®] solution (5 wt%, Dupont) was added into 1 mL of ethanol with ultrasonic for 15 min, then 5 mg of catalyst powder was added with ultrasonic for another 1 h to prepare the catalyst ink. Then 25 μ L of catalyst ink was applied to the glassy carbon disk surface with a micropipette to form a

uniform film. The RDE polarization plots were carried out in oxygen-saturated 0.5 M H₂SO₄ electrolyte with a potential step of 0.03 V and potential range from 0.8 V to -0.2 V at an electrode rotation speed of 1600 rpm. Before RDE tests, the electrocatalyst was scanned for several cycles between -0.2 V and 0.8 V with a scan rate of 50 mVs⁻¹ in argon-saturated 0.5 M H₂SO₄ electrolyte to activate the catalyst.

3. RESULTS AND DISCUSSION

3.1. BET analysis

The specific surface areas of XC72 and CNC are 237 and 398 m²g⁻¹ calculated by multi-point BET plots, respectively. The BJH pore size distribution shows that CNC has large mesopore size which is mainly distributed between 20~50 nm. Combine the following TEM images, the pore size can be originated from the inner diameter of CNC.

3.2. FTIR spectra

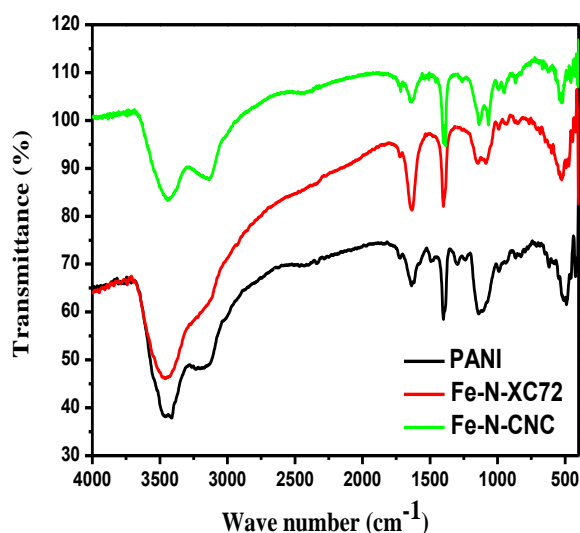


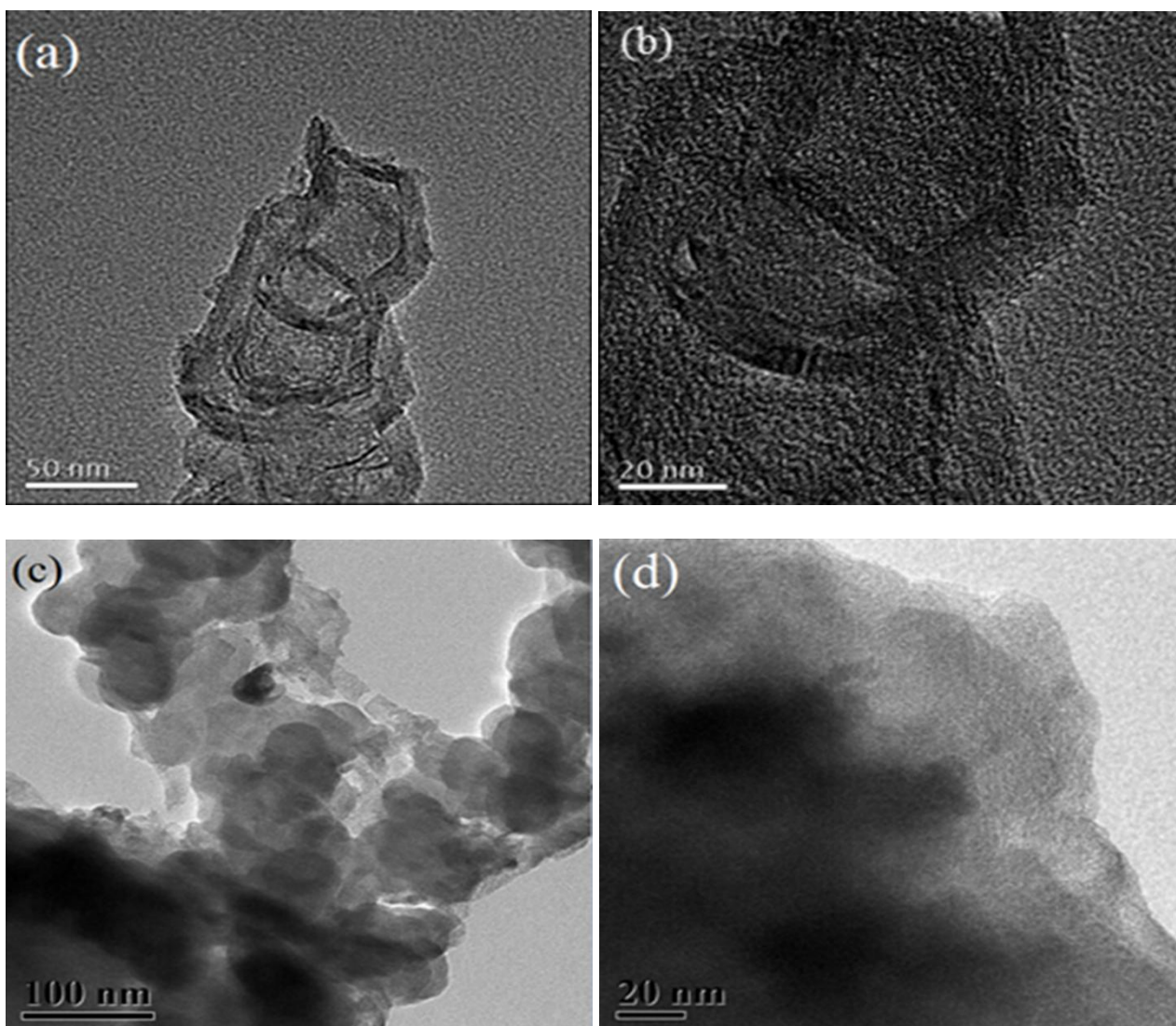
Figure 1. FTIR spectra of PANI, Fe-N-XC72 and Fe-N-CNC catalysts.

Fig.1 shows the FTIR spectra of PANI, Fe-N-XC72 and Fe-N-CNC catalysts. The spectrum corresponding to PANI shows various characteristic bands, C=C stretching mode of benzenoid and quinoidal moiety at 1410 and 1640 cm⁻¹ [15], N-H stretching mode at 3450 cm⁻¹, and N=Q=N (Q=quinone) at 1138 cm⁻¹, C-N stretching of secondary amine at 1295 cm⁻¹ [16]. Compared to the FTIR spectrum of PANI, some weak bands disappear in the FTIR spectra of Fe-N-XC72 and Fe-N-CNC catalysts, such as band at 1295 cm⁻¹ [17]. However, some new bands appear at 1080 cm⁻¹ referred

to a C-N stretching of aromatic amine [18]. It seems that main chains of polyaniline break into small species at 900 °C. Meanwhile, Fe-N-CNC catalyst exhibits more bands compared to Fe-N-XC72 catalyst, such as a band at 1266 cm^{-1} which could be referred to C-O stretching mode of surface functional group of CNC, which may be helpful to form more pyridinic and graphitic nitrogen.

3.3. TEM images

TEM images of CNC, Fe-N-XC72 and Fe-N-CNC catalysts are shown in Fig.2. CNC is mainly composed with coil-like nanostructures as shown in Fig.2 (a, b), the wall is ca. 5~15 nm in thick and the inner diameter is between 30~50 nm, which is in agreement with the BJH result, and the graphitic characteristic can be discerned from Fig.2 (b). This coil-like morphology and pore size can facilitate O_2 to get access to active sites. In Fig.2 (c, d), a narrow distribution of nanoparticles with an average diameter of 30-50 nm can be found in Fe-N-XC72 catalyst. No obviously graphitized carbon can be seen after PANI carbonized at 900 °C. CNC in Fe-N-CNC catalyst seems covered by PANI carbonization products as shown in Fig.2 (e, f).



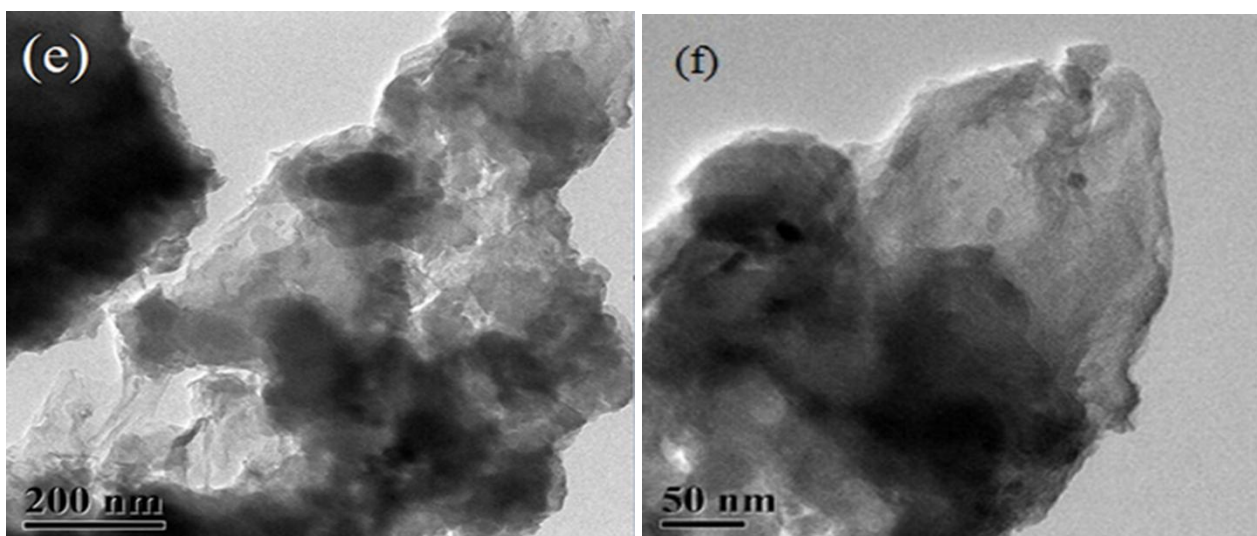


Figure 2. TEM images of carbon nanocoil (a, b), Fe-N-XC72 catalyst (c, d), and Fe-N-CNC catalyst (e, f).

Some tiny dark spots can be observed in Fig.2 (d, f), they could be metallic iron nanoparticles existed in Fe-N-CNC and Fe-N-XC72 catalysts which didn't get removed during acid leaching process.

3.4. XPS analysis

Fig.3 shows XPS survey spectra of Fe-N-XC72 and Fe-N-CNC catalysts. It reveals that both catalysts are mainly composed of carbon (C1s=284.5 eV) and oxygen (O1s=532.0 eV), a small amount of nitrogen (N1s=400.1 eV), and a trace of iron (Fe2p=710eV). Fe2p spectra of two catalysts are shown in Fig.4. Binding energy at 707.1-708.7 eV and 710.8-711.8 eV are respectively ascribed to Fe^{2+} and Fe^{3+} [19], and there is no big difference of iron content for the two catalysts. N1s spectra of Fe-N-CNC and Fe-N-XC72 catalysts are shown in the Fig.5, three types of nitrogen can be fitted: pyridinic nitrogen at 398.8 eV, pyrrolic nitrogen at 400.1 eV, and graphitic nitrogen at 401.4 eV [20, 21]. When the nitrogen precursors are pyrolyzed above 700 °C, nitrogen atoms can incorporate into carbon matrix to replace carbon atoms at different sites and form different types of nitrogen [22]. Pyridinic nitrogen is nitrogen atoms doped at the edge of the carbon layers, and graphitic nitrogen is nitrogen atoms doped inside a carbon layer. The nitrogen atoms doped into a pentagon structure could form pyrrolic nitrogen [23].

By qualitatively accumulate the respective area of three types nitrogen in the XPS spectra, atomic ratio of pyridinic nitrogen, pyrrolic nitrogen, and graphitic nitrogen were calculated and listed in Table 1. Comparing with the Fe-N-XC72, the Fe-N-CNC has higher content of pyridinic nitrogen and graphitic nitrogen, which are considered to have a correlation with a better ORR activity, but lower pyrrolic nitrogen which supposed to contribute no ORR activity [5]. The relative contents of total N species and C species have also been determined, and N/C ratio of Fe-N-XC72 is higher than that of Fe-N-CNC. Combine the ORR activity below, Fe-N-CNC catalyst displays better ORR activity,

indicating that the type of nitrogen incorporating in carbon is far more important than the total content of nitrogen.

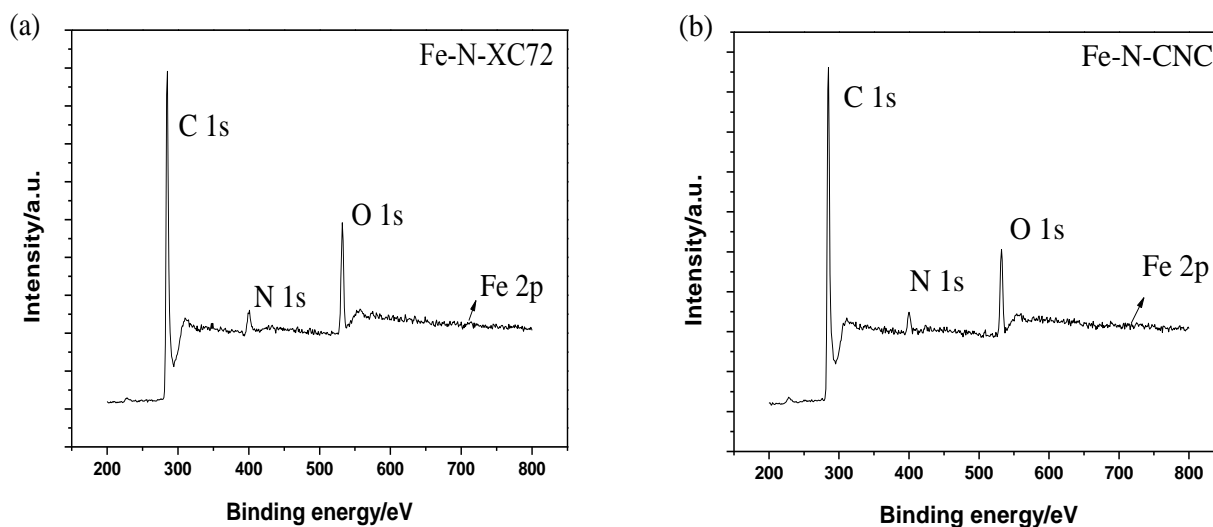


Figure 3. XPS spectra of catalysts Fe-N-XC72 (a) and Fe-N-CNC (b).

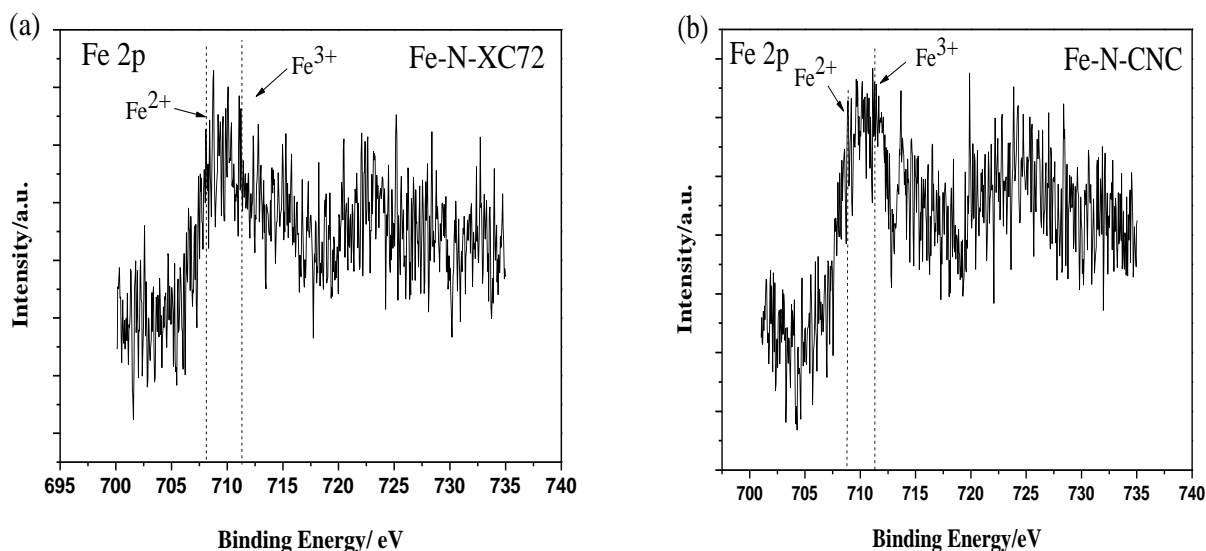


Figure 4. Fe 2p XPS spectra of catalysts Fe-N-XC72 (a) and Fe-N-CNC (b).

There is no doubt that nitrogen plays an important role in such nitrogen-doping catalysts. But the centre of catalytic sites of these Fe-N-C NPMCs is still a topic of debate [6, 10, 24]. One viewpoint on the role of Fe is that Fe species is not considered as an active site, but as a catalyst to generate active sites for ORR [24, 25], such as Dodelet group's opinion. However, some research groups claimed that Fe species coordinated with nitrogen (Fe-N₄/C) serve as highly active sites to catalyze oxygen reduction reaction, and this Fe/N/C catalytic site is composed of an iron cation coordinated with pyridinic nitrogen attached to the edges of two graphitic sheets [6, 26, 27].

Although pyridinic and graphitic nitrogen are considered as ORR active sites widely, the attempts to elucidate the role of Fe in such Fe-N-XC72 catalysts are necessary. A pair of well-identified $\text{Fe}^{2+}/\text{Fe}^{3+}$ redox peaks was observed in later cyclic voltammogram curves, indicating that Fe may be probably presented in the form of Fe-N_x . Thus we assume that pyridinic and graphitic nitrogen coordinated with iron to form Fe-N_x are the active sites to catalyze ORR in such iron-based nitrogen-doped catalysts.

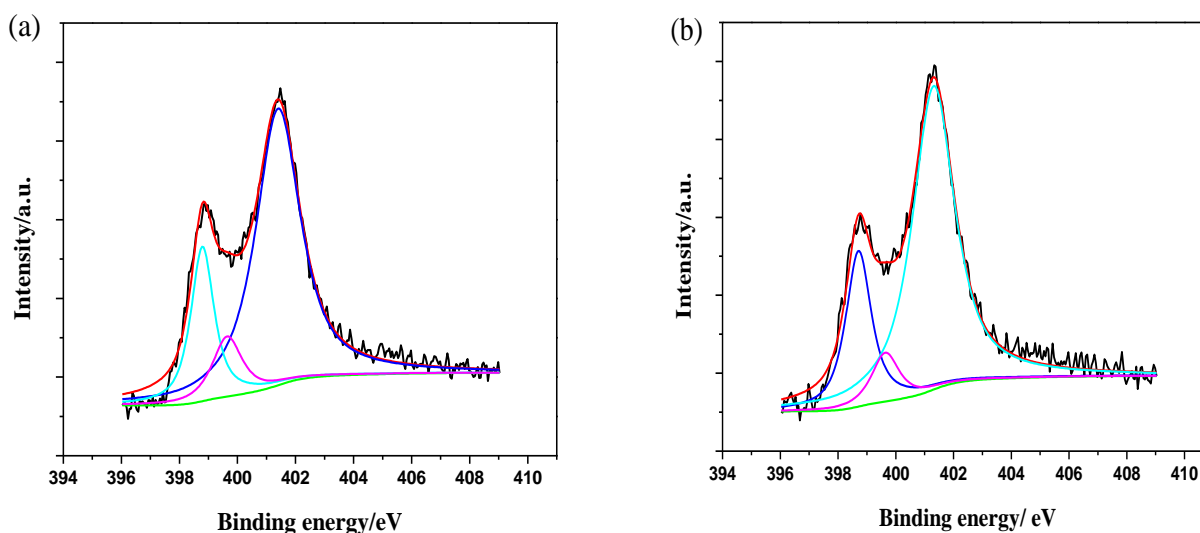


Figure 5. N1s XPS spectra of catalysts Fe-N-XC72 (a) and Fe-N-CNC (b).

Table 1. Different types of N species and N/C atomic ratios derived from XPS analysis of Fe-N-XC72 and Fe-N-CNC catalysts.

Sample	$N_{\text{pyridinic}}$	N_{pyrrolic}	$N_{\text{graphitic}}$	N/C
Fe-N-XC72	0.35	0.24	0.41	0.063
Fe-N-CNC	0.39	0.18	0.43	0.052

3.5. Electrochemical test and ORR Performance

Cyclic voltammograms of Fe-N-XC72 and Fe-N-CNC in Ar-saturated H_2SO_4 solution are shown in the Fig.6. In comparison with Fe-N-XC72 catalyst, Fe-N-CNC catalyst exhibits a larger specific surface area. A pair of well-identified redox peaks is revealed for both Fe-N-CNC and Fe-N-XC72 catalysts, which is related to the $\text{Fe}^{3+}/\text{Fe}^{2+}$ redox behavior [7]. The activities for ORR of these iron-based nitrogen-doped catalysts prepared with different contents of Fe were studied using RDE test. Fig.7 shows the LSV results. To investigate the role of iron species, Fe-N-C catalysts with nominal contents of Fe varied from 1 to 7 wt% were studied. As shown in the Fig.7, for both Fe-N-

XC72 and Fe-N-CNC catalysts, the activity for ORR increases with Fe content from 1 to 5 wt%, and starts to decrease from 7 wt% Fe. Here we can conclude that Fe is a critical factor for ORR activity of these nitrogen doped metal catalysts and the optimum iron content is 5wt%. Fig.8 shows the LSV curves of Fe-N-CNC and Fe-N-XC72 catalysts with Fe content of 5 wt%. Compared with Fe-N-XC72 catalyst, Fe-N-CNC catalyst exhibited 20 mV and 30 mV more positive onset potential and half-wave potential, respectively, indicating that Fe-N-CNC catalyst possessed a better ORR catalytic activity. We concluded that the enhancement of activity for ORR is related to the coil-like structure and more favorable nitrogen type of Fe-N-CNC catalyst which is beneficial to increase more active sites [5, 28].

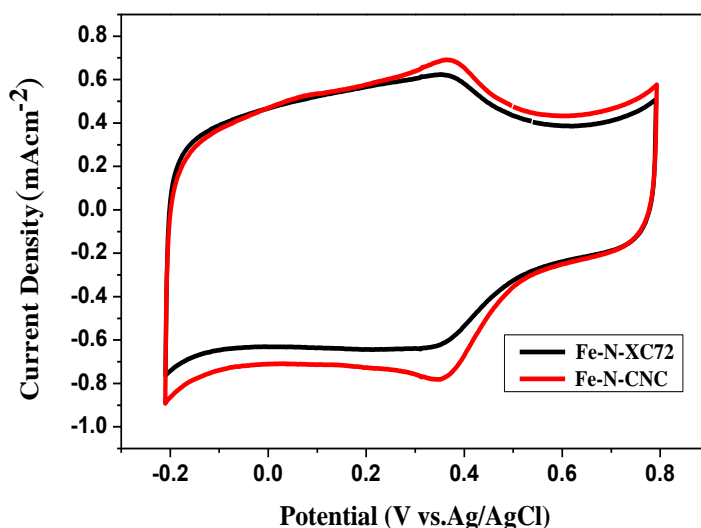


Figure 6. Cyclic voltammograms of Fe-N-XC72 and Fe-N-CNC catalysts in Ar-saturated 0.5 M H₂SO₄ solution with scan rate of 10 mV s⁻¹.

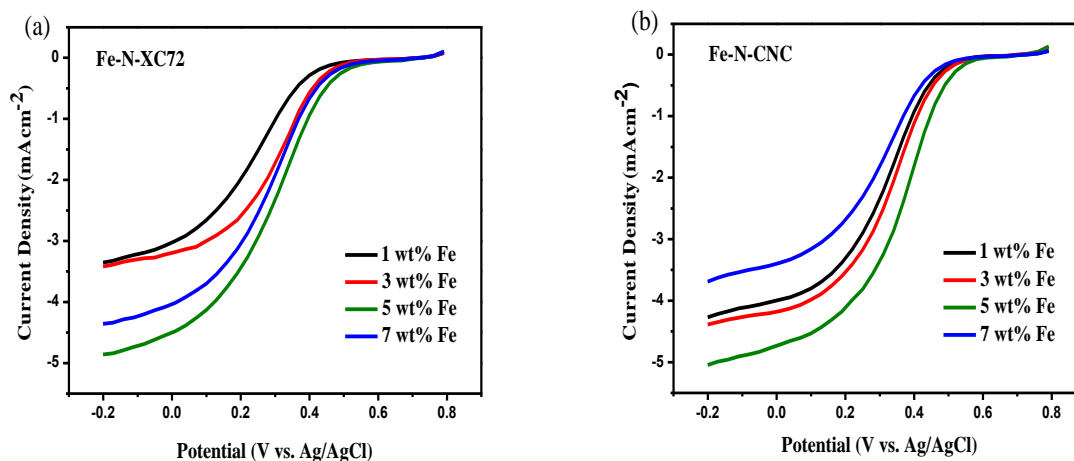


Figure 7. LSV curves of Fe-N-XC72 (a) and Fe-N-CNC (b) catalysts prepared with different nominal Fe contents.

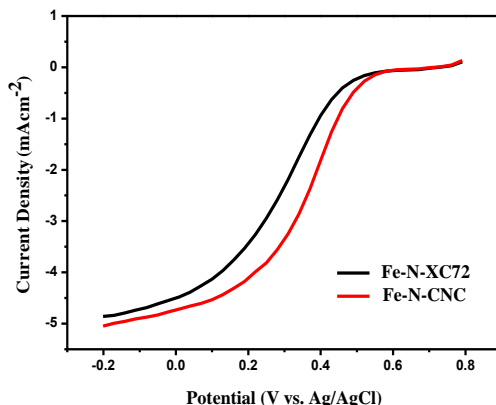


Figure 8. LSV curves of Fe-N-XC72 and Fe-N-CNC catalyst with 5 wt% Fe content.

3.6. ORR stability

The stability of such nitrogen-doped catalysts in PEMFC is another focus. In our work, the stability of Fe-N-CNC and Fe-N-XC72 catalysts were tested using LSV measurements with a scan rate of 50 mVs^{-1} between -0.2 and 0.8 V to study the activity before and after 1000 CV cycles. The ORR polarization plots measured with Fe-N-XC72 and Fe-N-CNC catalysts were recorded in Fig.9. The difference in half-wave potential before and after 1000 cycles is 20 mV for Fe-N-CNC catalyst, but 40 mV for Fe-N-XC72, indicating that the Fe-N-CNC catalyst is more stable than the Fe-N-XC72 catalyst under identical test conditions. The special structure of CNC which constructs a three-dimensional framework played an important role in the improvement of stability. It can provide a well-maintained three-phase interface which can facilitate the transportation of oxygen and electron/proton transfer. On the other hand, CNC with large specific surface area offers more active sites and uniform active site distribution which is beneficial for the stability of catalyst.

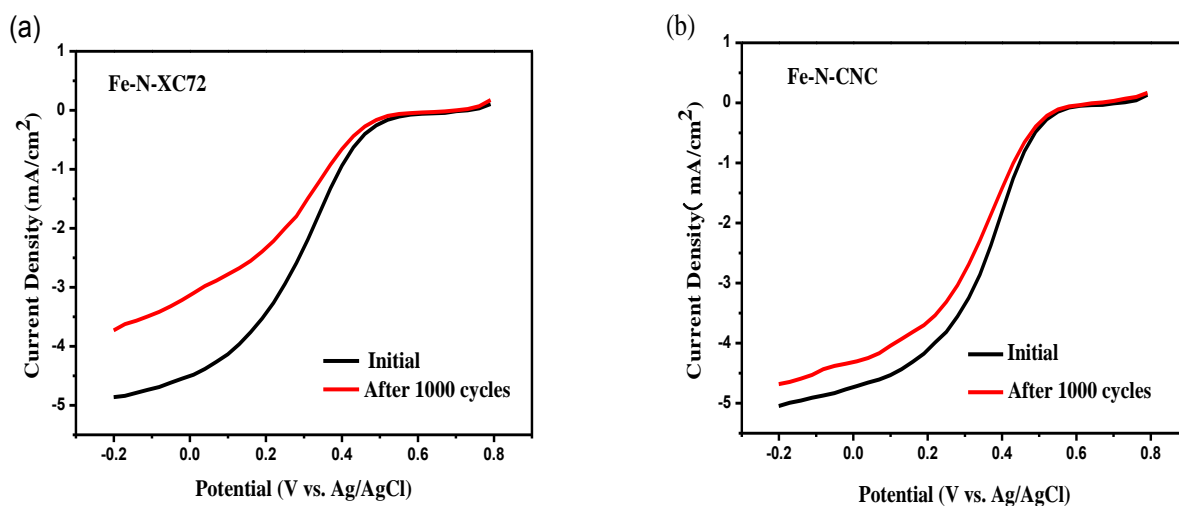


Figure 9. LSV curves of Fe-N-XC72 (a) catalyst and Fe-N-CNC (b) catalyst before and after 1000 cycles.

3.7. Discussion

The CNC with large specific surface area of $398 \text{ m}^2 \text{ g}^{-1}$ was synthesized by heat-treatment of resorcinol and formaldehyde resin in the presence of silicon. The three-dimensional structure observed by TEM images was beneficial to the increase of active sites density and quantity, the transportation of oxygen, and the improvement of ORR activity and stability of catalysts when CNC was used as carbon support to prepare catalysts. The importance of carbon support with large specific surface area and unique structure was concluded by Wu [12], which is consistent with our group's opinion. Furthermore, a pair of well-identified $\text{Fe}^{2+}/\text{Fe}^{3+}$ redox peaks was observed in cyclic voltammogram curves, indicating that Fe may be probably presented in the form of Fe-N_x . Thus we assume that pyridinic and graphitic nitrogen coordinated with iron to form Fe-N_x are the active sites to catalyze ORR in such iron-based nitrogen-doped catalysts, which is same with Dodelet's opinion [26]. The excellent activity and stability of Fe-N-CNC catalyst supported by CNC will contribute to the development of NPMCs.

4. CONCLUSIONS

Iron species is important for ORR activity, and the optimal Fe content for Fe-N-XC72 and Fe-N-CNC catalysts is 5 wt%. CNC supported Fe-N-CNC catalyst demonstrates better ORR activity and stability as compared to XC72 supported Fe-N-XC72 catalyst due to CNC with advantages of larger specific surface area, higher graphitic characteristic and unique morphology. Its advantages facilitate oxygen reduction reaction, and make it more suitable as an electrocatalyst support.

ACKNOWLEDGEMENTS

This work was supported by Scientific Research Foundation for Returned Scholars, Ministry of Education of China, International Technology Collaboration of Chengdu Science and Technology Division, the Open Project from State Key Lab of Catalysis (N-14-1), the Technology Project of Education Department of Sichuan Province (13ZA0193).

References

1. Z. Chen, D. Higgins and A. Yu, *Energ. Environ. Sci.*, 4 (2011) 3167
2. N. A. Karim and S. K. Kamarudin, *Appl. Energ.*, 103 (2013) 212
3. J. Zhang, S. H. Tang and L. Y. Liao, *Chin. J. Catal.*, 34 (2013) 1051
4. R. Jasinski, *Nature*, 201 (1964) 1212
5. P. H. Matter, L. Zhang and U. S. Ozkan, *J. Catal.*, 239 (2006) 83-96
6. M. Lefèvre, E. Proietti and F. Jaouen, *Science*, 324 (2009) 71
7. G. Wu, K. L. More and C. M. Johnston, *Science*, 332 (2011) 443
8. S. J. Kim, K. S. Nahm and P. Kim, *Catal. Lett.*, 142 (2012) 1244
9. H. W. Liang and W. Wei, *J. Am. Chem. Soc.*, 135 (2013) 16002
10. Z. Mo, H. Peng and H. Liang, *Electrochim. Acta*, 99 (2013) 30
11. G. Wu, C. M. Johnston and N. H. Mack, *J. Mater. Chem.*, 21 (2011) 11392
12. G. Wu, K. L. More and P. Xu, *Chem. Commun.*, 49 (2013) 3291

13. T. Hyeon, S. Han and Y. E. Sung, *Angew. Chem.*, 115 (2003) 4488.
14. J. Zhang and S. H. Tang, *J. Power Sources*, 267 (2014) 706
15. A. Sumboja, C.Y. Foo and J. Yan, *J Mater. Chem.*, 22 (2012) 23921
16. K. Mohd, J. S. Jose and A. Milton, *J Mater. Chem.*, 22 (2012) 11340
17. J. Luo, S. Jiang and R. Liu, *Electrochim. Acta.* 96 (2013) 103
18. S. Sultana and M. Muneer, *J. Mater. Sci. Technol.*, 9 (2013) 795
19. X. Fu, Y. Liu and X. Cao, *Appl. Catal. B-Environ.*, 130 (2013) 143
20. D. H. Lee, W. J. Lee and W. J. Lee, *Phys. Rev. Lett.*, 106 (2011)175502
21. Z. Chen, D. Higgins and Z. Chen, *Carbon*, 48 (2010) 3057
22. G. Wu, M. Nelson and S. Ma, *Carbon*, 49 (2011) 3972
23. J. R. Pels, F. Kapteijn and J. A. Moulijn, *Carbon*, 33 (1995) 1641
24. V. Nallathambi, J. W. Lee and S. P. Kumaraguru, *J. Power Sources*, 183 (2008) 34
25. P. H. Matter, E. Wang and M. Arias, *J. Phys. Chem. B*, 110 (2006) 18374
26. F. Jaouen, M. Lefèvre and J. P. Dodelet, *J. Phys. Chem. B*, 110 (2006) 5553
27. F. Charretier, F. Jaouen and S. Ruggeri, *Electrochim. Acta*, 53 (2008) 2925
28. X. Wang, J. S. Lee and Q. Zhu, *Chem. Mater.*, 22 (2010) 2178

© 2015 The Authors. Published by ESG (www.electrochemsci.org). This article is an open access article distributed under the terms and conditions of the Creative Commons Attribution license (<http://creativecommons.org/licenses/by/4.0/>).